Variational Calculations of Nuclei with Low-Momentum Potentials

S.K. Bogner and R.J. Furnstahl

Department of Physics, The Ohio State University, Columbus, OH 43210

Abstract

Variational calculations of the deuteron and the triton illustrate that simple wave function ansätze become more effective after evolving the nucleon-nucleon potential to lower momentum ("$V_{\mathrm{low}\,k}$"). This is consistent with many-body wave functions becoming much less correlated at lower cutoffs, as shown by two-particle wave functions and pair-distribution functions in nuclear matter. These results motivate a program to explore variational many-body calculations of binding energies and other low-energy nuclear properties using low-momentum potentials.

1 Introduction

Variational many-body calculations rely on being able to devise and optimize sufficiently rich wave function ansätze. The strong short-range repulsion and tensor forces of conventional nucleon-nucleon potentials that fit phase-shift data necessitate complicated, highly correlated trial wave functions, which limits the effectiveness of the variational approach. Even large-scale calculations of light nuclei using variational Monte Carlo (VMC) achieve accuracy only at the five percent level [1] and Green's function Monte Carlo (GFMC) is needed to evolve the wave functions [2]. Recent results with low-momentum potentials, however, suggest that more effective variational calculations should be possible [3].

The nonperturbative nature of conventional inter-nucleon interactions can be radically modified by using the renormalization group to lower the momentum cutoff of a two-nucleon potential [4]. For low-momentum interactions with cutoffs around $2\,\mathrm{fm}^{-1}$, the softened potential combined with Pauli blocking

Email addresses: bogner@mps.ohio-state.edu (S.K. Bogner), furnstahl.1@osu.edu (R.J. Furnstahl).

leads to corrections in nuclear matter in the particle-particle channel that are well converged at second order in the potential. Calculations of nuclear matter using the low-momentum two-nucleon force $V_{\mathrm{low}\,k}$ with a corresponding leading-order three-nucleon (3N) force from chiral effective field theory (EFT) exhibit nuclear binding in the Hartree-Fock approximation, and become much less cutoff dependent upon adding the dominant second-order contributions. At the lower cutoffs, the iterated tensor interaction in the two-body sector does not play a major role in nuclear saturation, in contrast to conventional wisdom. Thus, the relative importance of contributions to observables from the tensor force or from three-body forces is strongly scale or resolution dependent.

Similarly, the correlations in many-body wave functions will exhibit significant resolution dependence. The dominance of Hartree-Fock and the onset of perturbative convergence in the particle-particle channel at smaller cutoffs implies that the corresponding wave functions are much less correlated than those associated with conventional potentials. This has the practical consequence that variational calculations should be effective with much simpler ansätze. In this letter, we illustrate this simplicity through variational calculations of the deuteron and triton, and by examining the pair-distribution and two-particle wave functions in nuclear matter at empirical saturation density. We are *not* trying at this stage to optimize the variational approach for low-momentum potentials. Rather our goal is to motivate a program to re-examine the application of variational methods to binding energies and other low-energy properties of nuclei using low-momentum interactions.

The construction of $V_{\mathrm{low}\,k}$ is well documented in Refs. [5,6], where it is shown that either renormalization-group equations or Lee-Suzuki transformations can be used. Here we employ the latter, which provide a convenient formalism to evolve consistent operators beyond the Hamiltonian. In the notation of Ref. [7,8], the evolution of an operator $\widehat{O}$ from a momentum cutoff Λ_0 to $\Lambda < \Lambda_0$ is given by

$$\widehat{O}(\Lambda) = \frac{1}{\sqrt{P+\omega^\dagger\omega}}(P+\omega^\dagger)\widehat{O}(\Lambda_0)(P+\omega)\frac{1}{\sqrt{P+\omega^\dagger\omega}}, \qquad (1)$$

where the operator $\omega = Q\omega P$ parameterizes the Lee-Suzuki transformation, the projection operator P projects onto relative momenta $k \leq \Lambda$, and Q projects onto $\Lambda < k \leq \Lambda_0$. In the case of the evolved Hamiltonian it is convenient to define $V_{\mathrm{low}\,k}(\Lambda) \equiv H(\Lambda) - T$, where T is the "bare" kinetic energy operator. By construction, two-body bound-state properties and phaseshifts are preserved for external relative momenta up to the cutoff. Three- and many-body observables require the consistent addition of a three-body force to remove cutoff dependence [6].

We will show results starting from the Argonne v_{18} potential [9], since it is used in almost all modern VMC and GFMC calculations. However, for cutoffs

of $2\,\mathrm{fm}^{-1}$ or less, *all* bare potentials that reproduce nucleon-nucleon phase shifts up to 350 MeV lab energy, including EFT potentials at N3LO, collapse to the same $V_{\mathrm{low}\,k}$ [5]. Therefore, the pattern of results for the full cutoff range shown here does not vary significantly with different initial potentials.

Since $V_{\mathrm{low}\,k}$ is energy independent, variational calculations with $V_{\mathrm{low}\,k}$ proceed as described in ordinary quantum mechanics texts (e.g., without special normalizations as needed for energy-dependent potentials). That is, given a trial wave function ψ_{trial}, our variational estimate for the ground state energy at cutoff Λ is:

$$E_{\mathrm{var}}(\Lambda) = \frac{\langle\psi_{\mathrm{trial}}|T + V_{\mathrm{low}\,k}(\Lambda)|\psi_{\mathrm{trial}}\rangle}{\langle\psi_{\mathrm{trial}}|\psi_{\mathrm{trial}}\rangle} \ , \tag{2}$$

which we minimize with respect to the parameters in ψ_{trial}. Alternatively, we get a variational estimate by diagonalizing $T + V_{\mathrm{low}\,k}(\Lambda)$ in a truncated basis, where the trial wavefunction is a linear combination of the basis functions.

2 Deuteron

We start with a study of the deuteron binding energy. The philosophy is that for a weakly bound state one shouldn't need to work hard, so a simple, generic ansatz should work well. We test this as a function of the cutoff. Our first ansatz is adapted from the discussion of wave functions in momentum space given long ago by Salpeter [10], which motivates the (unnormalized) ${}^3S_1$ and ${}^3D_1$ trial functions for the deuteron (following the conventions of Ref. [11])

$$\psi_0(k) = \frac{1}{(k^2+\gamma^2)(k^2+\mu^2)} \ , \qquad \psi_2(k) = \frac{a\,k^2}{(k^2+\gamma^2)(k^2+\nu^2)^2} \ , \tag{3}$$

where γ, μ, ν, and a are variational parameters. Obviously we could extend this ansatz in many ways, but our point is to see how well we can do without having detailed knowledge about the wave function. The underlying physics implies that μ and ν should be roughly the inverse range of the interaction and γ should be close to $(-M_N E_d)^{1/2}$, where M_N is the mean neutron-proton mass and $E_d \approx -2.2246\,\mathrm{MeV}$ is the deuteron binding energy. Moreover, the cutoff in $V_{\mathrm{low}\,k}$ implies that the exact deuteron wave function does not contain high-momentum components. Therefore, the two-body trial wave functions considered contain the same cutoff on the relative momentum.

The best variational energy for Eq. (3) as a function of the cutoff is shown as the squares in Fig. 1. These estimates are not even bound for cutoffs above $\Lambda \approx 5\,\mathrm{fm}^{-1}$ (which includes the bare Argonne v_{18} potential) but rapidly improve as the cutoff is lowered further, reaching a minimum deviation of less than 3 keV around $\Lambda \approx 1.5\,\mathrm{fm}^{-1}$. We emphasize that the low-momentum potential really

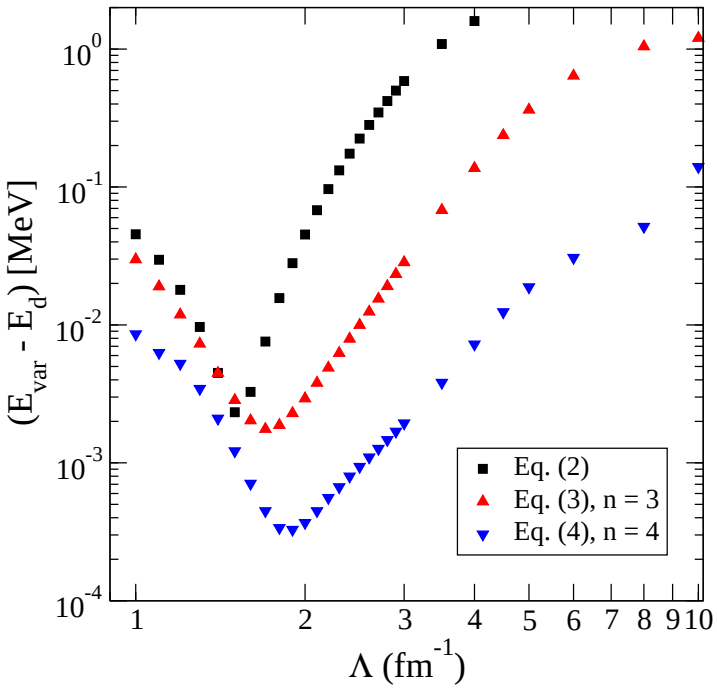

Fig. 1. Deviation from E_d of the best variational energy as a function of cutoff Λ for the wave function ansätze of Eqs. (3) and (4) with different numbers of terms.

does preserve the two-body observables; directly solving the momentum space Schrödinger equation with 40 gauss points yields the same deuteron binding energy as the bare potential to a fraction of an electron volt for all the cutoffs shown. But variational calculations with the lower cutoffs come much closer to this energy.

We can also adapt the form used for a high-accuracy representation of the deuteron wave function in Ref. [11] (and elsewhere) to see if the same pattern holds. Consider

$$\psi_0(k) = \sum_{j=1}^{n} \frac{C_j}{k^2 + m_j^2} \ , \qquad \psi_2(k) = \sum_{j=1}^{n} \frac{D_j}{k^2 + m_j^2} \ , \tag{4}$$

where the m_j are fixed in a geometric progression:

$$m_j = (-M_N E_d)^{1/2} + (j-1)m_0 \ , \quad \text{with } m_0 = 0.9\,\text{fm}^{-1} \ , \tag{5}$$

and we treat the C_j and D_j as variational parameters for a given value of n. (The very accurate *parameterization* of the deuteron wave function for the Bonn potential in Ref. [11] has $n = 11$ with some constraints on the C_j's and D_j's.) Since the variational coefficients appear linearly, we can simply diagonalize the Hamiltonian in the truncated basis of Eq. (4) to find the best estimate of the deuteron energy. For $n = 2$, the best estimate is about 5 keV above E_d at $\Lambda \approx 1.4\,\text{fm}^{-1}$ and is unbound above $6\,\text{fm}^{-1}$. By enlarging the basis ($n = 3$ and $n = 4$ are shown in Fig. 1) we find better estimates for all Λ, but the steep improvement remains with the minimum shifting gradually higher.

The success of simple ansätze for the deuteron at low cutoffs can be understood by looking at the corresponding wave functions. In Fig. 2, we show the exact deuteron wave functions in momentum space for a variety of cutoffs. The immediate source of the problem for a good energy estimate at higher cutoffs is the node in momentum space, which reflects the short-range correlations that are evident as a suppression of the coordinate-space wave function for $r < 1\,\mathrm{fm}^{-1}$ (see Fig. 3) [12]. This short-range/high-momentum behavior is increasingly resolved at higher cutoffs, which entails finer and finer cancellations in the variational integrals.

As suggested by the plots of the ${}^3S_1$ component $\psi_0(k)$ in Fig. 2 and the analogous behavior of the ${}^3D_1$ component $\psi_2(k)$, matrix elements of the operator $a^\dagger_{\mathbf{k}} a_{\mathbf{k}}$ (which are proportional to $|\psi_0(k)|^2 + |\psi_2(k)|^2$) change as Λ is lowered. This is neither surprising nor worrisome, since the momentum distribution defined by the "bare" $a^\dagger_{\mathbf{k}} a_{\mathbf{k}}$ operator is not an observable (see Ref. [13] for a detailed discussion), and more generally because operators beyond the Hamiltonian must also be evolved in order to give Λ independent expectation values [14]. However, as a test of our crude variational wave functions, it is instructive to start with this operator and a potential at a large cutoff Λ_0 (e.g., $10\,\mathrm{fm}^{-1}$) and evolve both down to Λ using Eq. (1). By construction, matrix elements with the exact wave functions as in Fig. 2 are unchanged even for $k > \Lambda$; we have verified this explicitly. One might worry that an intricate interplay of operator and wavefunction is needed to preserve the matrix element and this might be lost with a variational wave function, but this is not the case with low momentum interactions. For example, matrix elements of the evolved operator with the simple variational wave function of Eq. (3) for $\Lambda \approx 1.5\,\mathrm{fm}^{-1}$ (which gives the best energy estimate) underpredict the exact result by less than 4% for $k < 0.1\,\mathrm{fm}^{-1}$ and then closely reproduce it for all k up to $5\,\mathrm{fm}^{-1}$. This issue will be examined in more generality in future work.

3 Triton

Moving from the deuteron to the triton is a significant step in complexity, but we can still test fairly simply whether the basic deuteron results carry over by using a truncated harmonic oscillator basis for a variational calculation. The antisymmetric three-nucleon basis is generated from the Jacobi coordinate oscillator states [8]

$$|\,(nlsjt;\mathcal{N}\mathcal{L}\frac{1}{2}\mathcal{J}\frac{1}{2})JT\rangle, \tag{6}$$

where $(nlsjt)$ and $(\mathcal{N}\mathcal{L}\frac{1}{2}\mathcal{J}\frac{1}{2})$ are the quantum numbers corresponding to the two relative Jacobi coordinates [e.g., $\mathbf{k} = \frac{1}{2}(\mathbf{p}_1 - \mathbf{p}_2)$ and $\mathbf{q} = \frac{2}{3}(\mathbf{p}_3 - \frac{1}{2}(\mathbf{p}_1 + \mathbf{p}_2))$], and the basis is truncated according to the total number of oscillator quanta $N = (2n+l+2\mathcal{N}+\mathcal{L}) \leq N_{max}$. Diagonalizing the intrinsic Hamiltonian

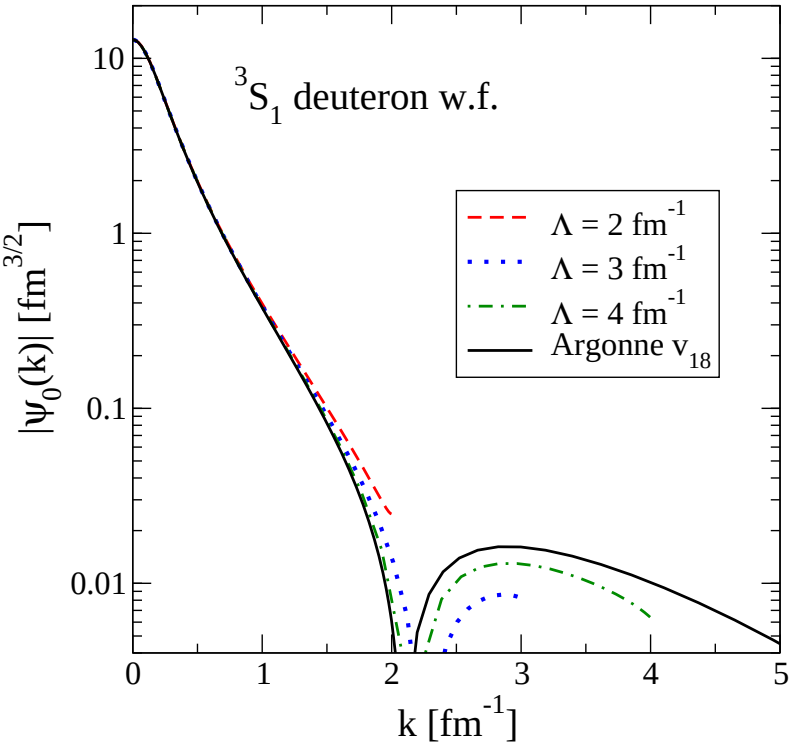

Fig. 2. Momentum-space $^3S_1$ deuteron wave function for a range of cutoffs and for the bare Argonne v_{18} potential.

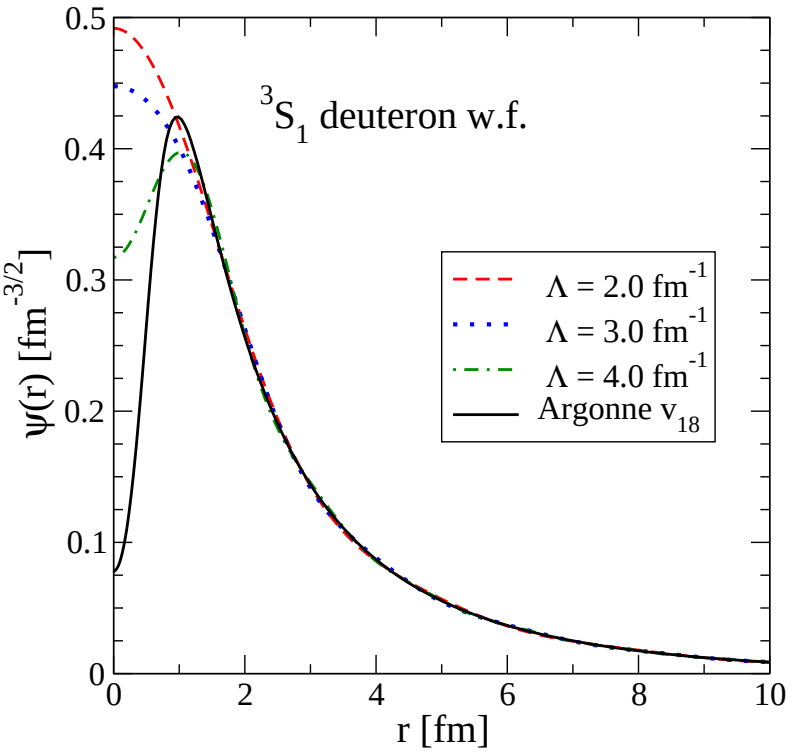

Fig. 3. Coordinate-space $^3S_1$ deuteron wave function for a range of cutoffs and for the bare Argonne v_{18} potential.

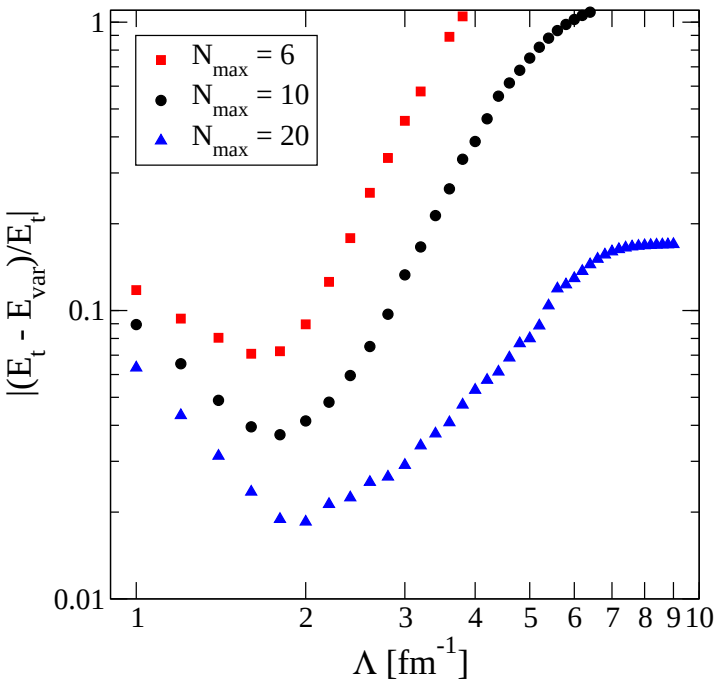

Fig. 4. Relative deviation of the variational energy from the Faddeev result for the triton (E_t) with two-body interactions only, as a function of cutoff Λ for several truncated oscillator basis sets.

in the truncated basis and minimizing with respect to the oscillator length parameter b provides a variational estimate to the true ground-state energy.

Results for the triton with two-body interactions only are shown in Fig. 4. Since the three-body contribution varies with the cutoff, the reference value for two-body alone varies as well. Therefore, the results are given at each Λ with respect to the exact Faddeev result [6] *at that* Λ, which we label E_t.

We see in the figure the same qualitative pattern as found for the deuteron. We can calibrate the efficacy of the harmonic oscillator basis at lower cutoffs by comparison to the calculation by Nunberg et al. [15], which used the Reid soft-core interaction (which actually has quite a repulsive core). Even using a basis with an additional nonlinear variational parameter compared to the current calculation, their predicted triton energy is not even negative until $N_{\max} \geq 12$ and the largest calculation with $N_{\max} = 28$ yields $E_t = -6.7\,\mathrm{MeV}$, which is extrapolated to $E_t = -7.3 \pm 0.2\,\mathrm{MeV}$ for $N_{\max} \to \infty$. That is, $N_{\max} = 28$ is still 600 keV above the converged result. In contrast, for $V_{\mathrm{low}\,k}$ with $\Lambda = 1.8\,\mathrm{fm}^{-1}$, the result for $N_{\max} = 6$ is already only 620 keV above the converged result, and this drops to 160 keV for $N_{\max} = 20$. [1]

[1] We anticipate even better variational convergence properties if one uses a smooth momentum cutoff in $V_{\mathrm{low}\,k}$.

4 Nuclear Matter

We are optimistic that the general pattern we have seen in simple two- and three-nucleon variational calculations will continue for heavier systems (and with the inclusion of the corresponding low-momentum three-body force), and that the variational improvement upon lowering the cutoff is universal. Our optimism is based on calculations of nuclear matter with low-momentum potentials, which are discussed in Ref. [4].

Two convenient measures of correlations in nuclear matter are the in-medium pair wave functions and the pair-distribution function. Working within the Brueckner approximation, the relative in-medium wave function for a pair of nucleons with total momentum $\mathbf{P}$ and relative momentum $\mathbf{k}$ is

$$|\,\Psi^{\mathbf{P}}_{\mathbf{k}}\rangle = |\,\mathbf{k}\rangle + \frac{Q}{\omega - H_0} G^{\mathbf{P}}(\omega)\,|\,\mathbf{k}\rangle, \tag{7}$$

where Q is the Pauli blocking operator and G is the usual Brueckner G matrix, which sums the in-medium particle-particle ladder diagrams. In the current calculation, all self-energy effects are neglected for simplicity, which corresponds to setting $\omega = k^2 + \frac{1}{4}P^2$ and using the pair kinetic energy operator for H_0. We stress that the overall pattern of our results are not changed by this assumption. At the same level of approximation, the pair-distribution function is given in terms of the coordinate-space pair wave functions [16],

$$g(r) = \sum_{ST} (2T+1)(2S+1) \sum_{|\frac{\mathbf{P}}{\mathbf{2}} \pm \mathbf{k}|}^{k_F} \left| \Psi^{\mathbf{P}}_{\mathbf{k}}(r; ST) \right|^2. \tag{8}$$

Physically, $g(r)$ corresponds to the correlation function for finding another nucleon a distance r from the first.

In Fig. 5 we show the ${}^3S_1$ wave function in the ${}^3S_1$–${}^3D_1$ coupled-channel for a pair of nucleons with $P = 0$ and $k = 0.1\,\mathrm{fm}^{-1}$, and in Fig. 6 the pair-distribution function in nuclear matter at empirical saturation density $k_\mathrm{F} = 1.35\,\mathrm{fm}^{-1}$. Unless otherwise noted, the curves include the dominant effects of the corresponding three-body force at each cutoff by converting the 3N vertex into a density-dependent two-body correction that is added to $V_{\mathrm{low}\,k}$, see Ref. [4] for details.

The two-particle wave functions and pair-distribution functions in nuclear matter exhibit the same promising features we found in the simpler two- and three-nucleon systems. Namely, the strong short-ranged correlations are "blurred out" as the interactions are evolved to lower momenta. This is clear for the two-particle wave function, where the "wound" resulting from the short-range repulsion is more pronounced at the higher cutoffs. Similar re-

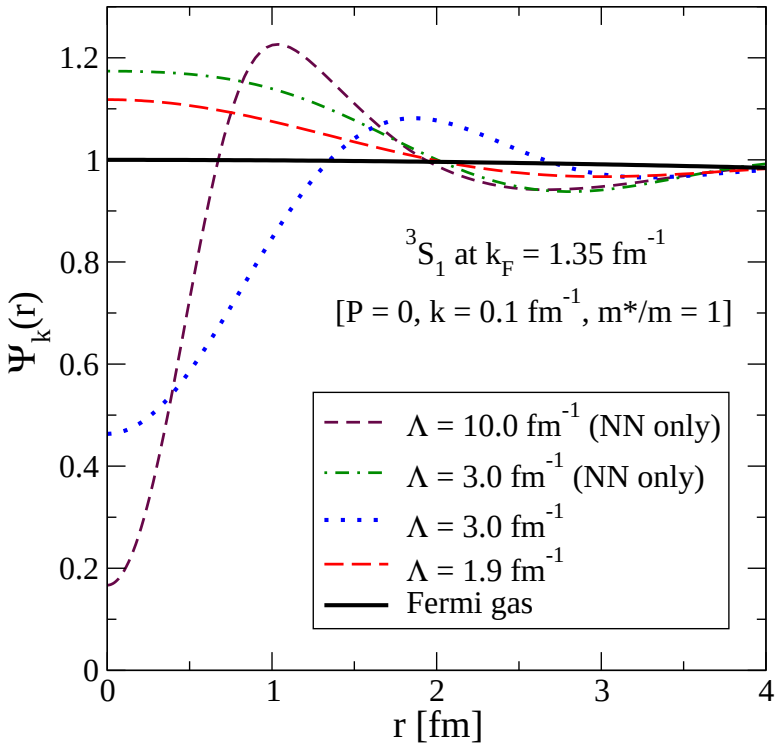

Fig. 5. Two-particle wave function for the ${}^3S_1$ channel in symmetric nuclear matter at $k_{\rm F} = 1.35\,{\rm fm}^{-1}$.

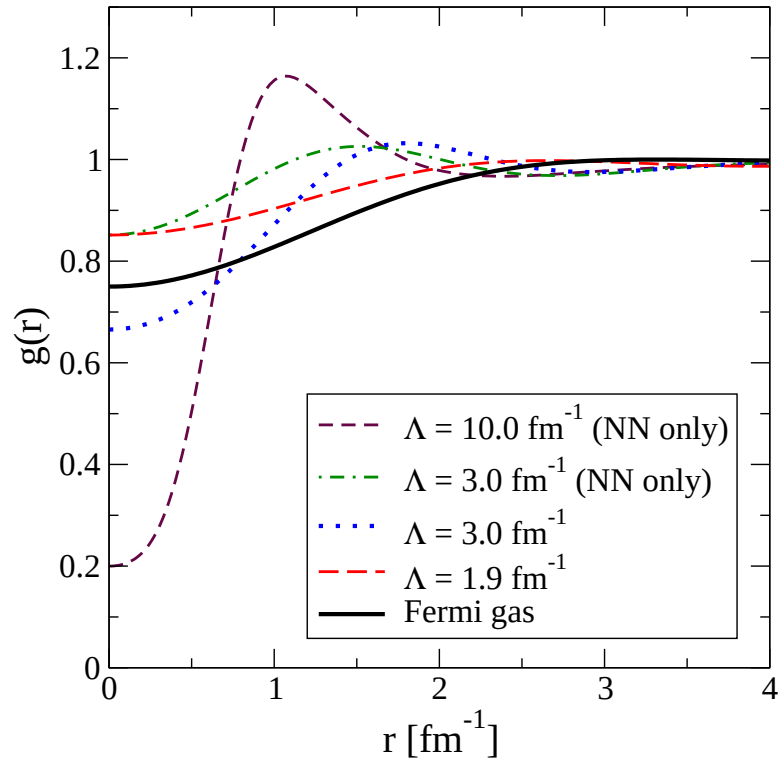

Fig. 6. Pair-distribution function in symmetric nuclear matter at $k_{\rm F} = 1.35\,{\rm fm}^{-1}$.

sults are found for the pair-distribution function, where $g(r)$ at smaller cutoffs has little short distance structure and lies fairly close to the Fermi gas (i.e., Hartree-Fock wave functions) values, where the correlations arise solely from Fermi statistics.

It is interesting to note that the correlations induced by the three-body force are significantly stronger at larger cutoffs. At $\Lambda = 3.0\,\mathrm{fm}^{-1}$, which is the largest cutoff at which the three-body force was fitted for $V_{\mathrm{low}\,k}$ [6], the pair-distribution function is suppressed at short distances (relative to the Fermi gas values) when the three-body force is included. In contrast, there is a slight *enhancement* in $g(r)$ at short distances when only the two-body $V_{\mathrm{low}\,k}$ is used.

One finds that the changes in $g(r)$ with and without the three-body force are much less severe at lower cutoffs. For example, at a cutoff of $\Lambda = 1.9\,\mathrm{fm}^{-1}$ one finds that $g(r = 0)$ decreases by only 0.1 when the three-body force is included, while the corresponding change for $\Lambda = 3.0\,\mathrm{fm}^{-1}$ is a factor of two larger. This is consistent with the results of Ref. [6], where it was shown that at smaller cutoffs the three-body force can be accurately treated in perturbation theory for the triton and alpha particle ground state energies.

As we saw for the deuteron, these plots show that short-range correlations do not need to be explicit in the wave functions when calculating low-energy/low-momentum observables up to nuclear matter densities. The key point is that lowering the resolution makes calculations *simpler*, more efficient, and less model-dependent.

5 Conclusions

In summary, the direct evidence from the deuteron and triton, coupled with the rapid convergence of the particle-particle channel observed in nuclear matter, imply that low-momentum potentials with $\Lambda \approx 2\,\mathrm{fm}^{-1}$ will be much more effective for few-body and many-body variational calculations than any conventional large-cutoff potential. Furthermore, even chiral EFT potentials, which are themselves low-momentum potentials compared to conventional potentials such as Bonn, Nijmegen, or Argonne, can be made more effective by running the cutoff lower. The general idea is to take the EFT cutoff as large as possible (i.e., in the vicinity of the *breakdown* scale of the chiral EFT, which presumably is $3\,\mathrm{fm}^{-1}$ or higher), in order to minimize the truncation error [17]. The evolution to lower cutoffs induces the higher-order short-ranged operators that maintain the same truncation error in observables as at the higher cutoff.

To take advantage of these observations, variational Monte Carlo (VMC) is attractive for its basic simplicity, the upper-bound property of the energy es-

timates, and the absence of the fermion sign problem. Variational calculations with conventional (large cutoff) potentials are performed in coordinate space, where the strong correlations are most naturally encoded in trial wave functions [1]. In fact, most calculations of this sort have used some variety of the Argonne potential, which was designed for this purpose and for subsequent GFMC calculations built on the variational results (local and operator based) [1,2].

Based on our results here, we anticipate more efficient variational results for low-momentum interactions, with the added advantage of being able to vary the cutoff as a tool to optimize and probe the quality of the solution. We have no restriction to coordinate space and, indeed, we will first try to develop Monte Carlo calculations for light nuclei directly in momentum space. Furthermore, we can avoid the problem of constructing consistent, model-independent operators for conventional potentials by evolving to low momentum the potential and operators from chiral EFT. More generally, since Hartree-Fock is a reasonable starting point for many-body calculations, the large arsenal of techniques developed for the Coulomb many-body problem becomes available and should be explored as well.

Acknowledgements

We thank Achim Schwenk and Thomas Duguet for useful comments and discussions. This work was supported in part by the National Science Foundation under Grant No. PHY–0354916.

References

[1] R.B. Wiringa, Phys. Rev. **C43** (1991) 1585;
S.C. Pieper, R.B. Wiringa, and V.R. Pandharipande, Phys. Rev. **C46** (1992) 1741.

[2] S.C. Pieper and R.B. Wiringa, Ann. Rev. Nucl. Part. Sci. **51** (2001) 53;
S.C. Pieper, R.B. Wiringa and J. Carlson, Phys. Rev. **C70** (2004) 054325.

[3] S. K. Bogner, T. T. S. Kuo, L. Coraggio, A. Covello, N. Itaco, Phys. Rev. **C65** (2002) 051301(R);
L. Coraggio, N. Itaco, A. Covello, A. Gargano, T. T. S. Kuo, Phys. Rev. **C68** (2003) 034320;
A. Schwenk, A. P. Zuker, arXiv:nucl-th/0501038.

[4] S. K. Bogner, A. Schwenk, R. J. Furnstahl and A. Nogga, arXiv:nucl-th/0504043.

[5] S.K. Bogner, T.T.S. Kuo, A. Schwenk, D.R. Entem and R. Machleidt, Phys. Lett. **B576** (2003) 265;
S.K. Bogner, T.T.S. Kuo and A. Schwenk, Phys. Rept. **386** (2003) 1.

[6] A. Nogga, S.K. Bogner and A. Schwenk, Phys. Rev. **C70** (2004) 061002(R).

[7] I. Stetcu, B.R. Barrett, P. Navratil, J.P. Vary Phys. Rev. **C71** (2005) 044325.

[8] P. Navratil, G.P. Kamuntavicius, B.R. Barrett, Phys. Rev. **C61** (2000) 044001.

[9] R.B. Wiringa, V.G.J. Stoks and R. Schiavilla, Phys. Rev. **C51** (1995) 38.

[10] E. E. Salpeter, Phys. Rev. **84** (1951) 1226.

[11] R. Machleidt, Phys. Rev. **C63** (2001) 024001.

[12] M. Garcon and J. W. Van Orden, Adv. Nucl. Phys. **26**, 293 (2001) [arXiv:nucl-th/0102049].

[13] R.J. Furnstahl and H.-W. Hammer, Phys. Lett. **B531** (2002) 203.

[14] W.C. Haxton and C.-L. Song, Phys. Rev. Lett. **84** (2000) 5484.

[15] P. Nunberg, D. Prosperi, and E. Pace, Nucl. Phys. **A285** (1977) 58.

[16] D. N. Lowy and G. E. Brown, Phys. Rev. **B12** (1975) 2138.

[17] G.P. Lepage, "How to Renormalize the Schrödinger Equation", Lectures given at 9th Jorge Andre Swieca Summer School: Particles and Fields, Sao Paulo, Brazil, February, 1997, nucl-th/9706029.